CHEMIJA. 2016. Vol. 27. No. 2. P. 93–99

Relation between spectral and spatial properties of gold nanoclusters modified by the morpholine ligand

Akvilė Šlėktaitė[1, 2],

Reda Kubiliūtė[1],

Deividas Sabonis[1, 2],

Ričardas Rotomskis[1, 2]

[1] *Biomedical Physics Laboratory, National Cancer Institute, Baublio St. 3b, LT-08406 Vilnius, Lithuania*

[2] *Biophotonics Group of Laser Research Center, Vilnius University, Saulėtekio Ave. 9, Bldg. 3, LT-10222 Vilnius, Lithuania*

Recently, gold nanoparticles have received the most attention due to the features and possible applications of their size dependent surface plasmon resonance, which disappears for nanoparticles less than 2 nm in size, that are called gold nanoclusters. Gold nanoclusters, composed of only several to tens of atoms, exhibit molecule-like electronic transitions and size-dependent photoluminescence. This effect offers many possible applications including biological and biochemical sensors and fluorescent bioimaging. Here we report the study of the spectral properties of gold nanoclusters synthesized using a 2-(N-morpholino) ethanesulfonic acid as a capping agent, and their relation to the spatial characteristics of these clusters. We investigated spectral changes of nanoclusters under varying pH value and sample preparation methods and observed the highest photoluminescence intensity at pH 6.3. According to theoretical models we estimated that these particles are composed of 8 atoms, which form a three-dimensional pyramidal structure ($C2_V$). At pH 4.9–5.8 additional plasmonic gold nanoparticles were generated with the calculated size of about 20 nm.

Keywords: MES capped fluorescent nanoparticles, plasmon resonance, gold nanoclusters, spectral properties, pH

INTRODUCTION

New properties emerge when the size of a matter is reduced from the bulk to the nanometer scale. These new properties, including optical, magnetic, electronic, and structural, make nano-sized particles (generally 1–100 nm in diameter) very promising for a wide range of biomedical applications such as cellular imaging, molecular diagnostics and targeted therapy. In recent years gold nanoparticles have been brought to the forefront of cancer research because of their facile synthesis and surface modification, tuneable optical properties as well as excellent biocompatibility.

Most attention has been paid to the large spherical gold nanoparticles that display size dependent surface plasmon resonance (SPR) absorption [1], which is a coherent oscillation of the conduction band electrons excited by electromagnetic radiation. This effect offers many possible applications including biological and biochemical sensors and surface-enhanced spectroscopy [2]. The typical SPR absorption band is between 520 and 545 nm, but it can shift depending on the size, shape and the aggregation behaviour of the nanoparticles [3–5]. The intensity of SPR absorption varies as the third power of the nanoparticle size [6] and completely disappears for nanoparticles less than 2 nm in size, which are called gold nanoclusters (AuNCs).

Gold nanoclusters are assemblies of a small number (2–30) of gold atoms, typically no bigger than 2 nm in diameter. Such metal nanoclusters, composed of only several tens of atoms, exhibit molecule-like electronic transitions as the density of states is insufficient to merge the valence and conduction bands [7, 8]. At sizes comparable to the Fermi wavelength of an electron (~0.7 nm in the case of gold), optical properties are significantly modified and discrete nanocluster energy levels become accessible [9], from which size-dependent photoluminescence (PL) of AuNCs originates [10].

Currently, synthesis of photoluminescent AuNCs most commonly uses large molecules as templates or encapsulation agents, such as dendrimers, polymers and proteins [10–15]. However, these templates increase the overall size of the nanoclusters and make it difficult to determine their core size and the details of the nanocluster-ligand interaction. Also, large fluorescent tags can disrupt the marked biomolecules and cause artificial movement within the cells [10].

The solution to these shortcomings might be photoluminescent AuNCs synthesized using small molecule ligands such as 2-(N-morpholino)ethanesulfonic acid (MES), as was recently shown by Bao et al. [16]. MES is a highly water-soluble buffering agent with a pK_a value of 6.15 that has specifically

* Corresponding author. E-mail: akvile.slektaite@nvi.lt

been developed for biological research [17]. The weight of these molecules is only 195.2 Da which is almost the same as the weight of one gold atom (197 Da), therefore MES, as a surfactant, does not significantly increase the size of a nanocluster. During the synthesis process MES molecules act both as a reducing agent and as a stabilizer of resulting nanoclusters. These MES capped AuNCs have a particularly small size (less than 1 nm) that does not influence any functions of bio-units [18]. Therefore they can be successfully used for biological applications such as tracking various processes inside cells.

Currently, considerable research efforts are directed towards investigation of synthesis routs of fluorescent AuNCs capped with reactive molecules [19–22], their optical properties [22–25] and possible applications for material sensing [22, 24, 25], and fluorescence imaging [26, 27].

So far there are only few studies about the photoluminescent gold nanoclusters synthesized using MES [16, 18, 28–31]. Compared to semiconductor quantum dots which possess size-dependent fluorescence in cases where a particle size is smaller than the exciton Bohr radius, AuNCs do not contain toxic heavy metals. Though also depending on their size, AuNCs are a potential alternative to quantum dots as fluorescence labels. The PL properties of AuNCs make them potential labels for biologically motivated experiments as well as for optical biopsy of the cancer [32].

In this study we describe an easy synthesis route for water-soluble MES capped AuNCs, investigate their optical properties such as PL and absorption depending on the reaction mixture pH and the relation between their spectral and spatial features. Ultimately, our goal is to implement AuNCs in imaging applications, so we attempt to tune the chemical synthesis to produce stable photoluminescent nanoclusters with high PL efficiency and predicted photophysical properties. For this purpose we performed synthesis optimisation.

EXPERIMENTAL

Materials. $HAuCl_4$ (99.9% purity, Sigma-Aldrich, USA), MES (2-(N-morpholino) ethanesulfonic acid) (98% purity, Sigma-Aldrich, Germany), sodium hydroxide (Riedel-de Haen, Germany) were used as received. Ultrapure water (Millipore) was used to prepare all aqueous solutions.

Synthesis of MES-encapsulated AuNCs. Photoluminescent MES-encapsulated AuNCs were synthesized according to the previously reported procedure [16] with slight modifications and using different pH of a reaction mixture. Typically, AuNCs were synthesized by mixing a chloroauratic acid ($HAuCl_4$) aqueous solution (5.8 mM, 1 ml) with MES buffer (0.1 M, 5 ml). The mixture was then stirred in a thermostat at 37 °C temperature for 21 hours and 30 minutes. We used different pH values of the MES buffer (pH 4.9, pH 5.2, pH 5.5, pH 5.8, pH 6.1, pH 6.3, pH 6.5, pH 7 and pH 7.5) which were reached by adding NaOH at room temperature. The most intense PL was observed using the above-mentioned synthesis procedure at pH 6.3.

The reaction mixtures were subsequently investigated spectroscopically and additionally centrifuged (10,000 g for 30 min).

Instrumentation. Optical parameters of the reaction mixtures were observed using a spectrometer (Cary 50 VARIAN, Australia) and a fluorescence spectrometer (Cary Eclipse VARIAN, Australia).

The theoretical modelling of particle sizes was done using the MiePlot software. The Mie algorithm used in the MiePlot is based on the BHMIE code published by Bohren and Huffman [33]. The Mie theory is the default calculation method used in the MiePlot. It offers a rigorous solution to the extinction of plane electromagnetic waves from a homogenous sphere.

RESULTS AND DISSCUSION

The photoluminescence emission, excitation and absorption spectra of the synthesized MES capped AuNCs together with the absorption of initial synthesis components are shown in Fig. 1. The PL spectrum (excitation at 420 nm) has a single band with a maximum at 480 nm while the excitation spectrum exhibits the main band with the maximum at 420 nm and a band of lower intensity at 275 nm when measured at the emission maximum. However, the absorption spectrum of AuNCs does not correlate with the PL excitation spectrum and exhibits a band with the maximum at 291 nm with a shoulder at 336 nm in the presence of a weak absorption band in the longer wave region. No PL was detected under excitation at the bands that can be clearly seen in the absorption spectra (291, 336 and 475 nm).

This implies that during the synthesis reaction a heterogeneous product is produced and the absorption in the UV–Vis region relates to synthesized non-photoluminescent components.

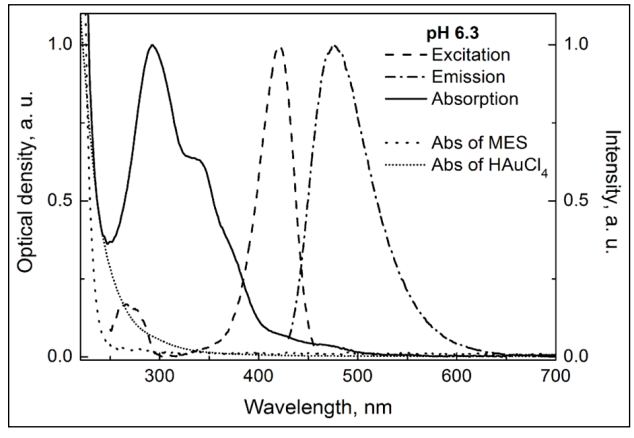

Fig. 1. The normalized PL excitation ($\lambda_{em} = 480$ nm), PL emission ($\lambda_{ex} = 420$ nm) and absorption spectra of AuNCs colloid at pH 6.3. Dotted lines represent the absorbance of MES and $HAuCl_4$

The synthesis of MES capped AuNCs at different pH values of an initial reaction mixture led to the observation that

PL intensity depends on the pH value of the reaction mixture (Fig. 2). At the acidic pH values (4.9–5.5) the PL signal is barely higher than the noise level. With an increasing pH of the reaction mixture, a higher PL intensity was detected and the maximum PL intensity was measured at pH 6.3, further increasing of pH led to a decrease of the PL intensity. The reaction mixture pH changes have influence on the PL intensity of gold nanoclusters, however, there are no other changes in the PL emission bands, as well as in the PL excitation bands, as it is seen from the normalized emission spectra at different pH presented in Fig. 3. Therefore, we infer that only one type of the photoluminescent AuNCs are synthesized at different pH values, and PL intensity changes reflect the different amount of gold clusters synthesized at different pH. The highest concentration of the photoluminescent gold nanoclusters was detected at pH 6.3.

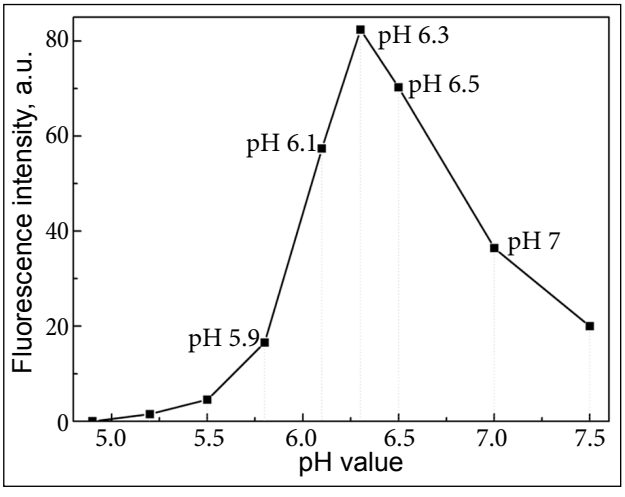

Fig. 2. The PL intensity of AuNCs dependence on the pH value of the reaction mixture at the same synthesis procedure and the same concentrations of reaction components

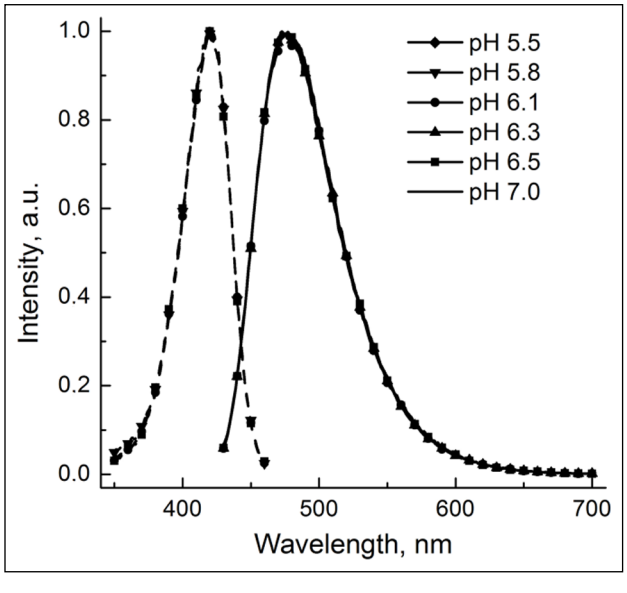

Fig. 3. The normalized PL emission (λ_{ex} = 420 nm, solid line) and PL excitation (λ_{em} = 480 nm, dashed line) spectra of AuNCs solutions at different pH values

A fully different picture was observed in the absorption spectra of gold nanoclusters under different pH (Fig. 4). In addition, the absorption features of colloids were measured after centrifugation – solid lines present the absorption spectra of centrifuged samples, dotted lines show the non-centrifuged samples. As is seen in Fig. 4, the number and position of the absorption peaks are highly depending on the pH value of the reaction solution. The absorption spectrum of AuNCs at pH 7.5 has a maximum at 307 nm with an insignificant shoulder at around 340 nm. This absorption band shifts to the blue region from 307 to 276 nm with a decreasing pH value until pH 4.9 is reached. Also, interplays of the absorption bands are detected at 340 and 370 nm. The band at 340 nm is the most prominent at pH 6.0, while the band at 370 nm becomes clearly visible at pH 4.9. In addition, a low intensity absorption band at 475 nm was detected in a neutral and slightly alkaline reaction mixture – at pH 7 and 7.5. As it is seen in Fig. 4, the absorption spectra of AuNCs colloids consist of superposition as a minimum of five absorption bands, the intensity and position of which depend on the pH value.

At acidic pH values the absorption spectra of centrifuged and non-centrifuged samples differ significantly in the long-wave region (Fig. 4). Distinct absorption bands with a maximum at 525 nm were observed, while at the lowest pH 4.9, even an additional absorption band with a peak at around 675 nm was detected. All particles responsible for these absorption bands could be easily removed by centrifugation (Fig. 4).

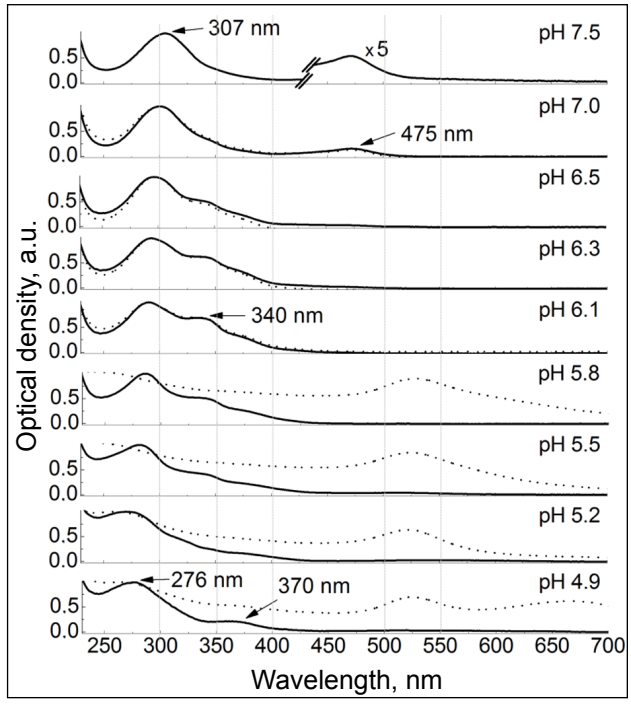

Fig. 4. The normalized absorption spectra of AuNCs colloids created at different pH values (a dotted line shows the absorption spectra of non-centrifuged samples, a solid line is those of centrifuged samples)

Photoluminescent MES capped AuNCs were synthesized according to the previously reported procedure [16] with slight modifications and using different pH values of the reaction mixture. Large gold nanoparticles are produced at the beginning of the synthesis and after a certain amount of time. According to the authors [29], these large nanoparticles start to decrease and photoluminescent nanoclusters are formed. The obtained results suggest that during the synthesis the largest amount of photoluminescent particles was generated in the reaction mixture of pH 6.3 (Fig. 2) and the PL intensity of that compound was 10 times greater than the one synthesized at pH 7 (suggested by An et al. [18]). The normalized PL emission and excitation spectra of different pH values overlap perfectly (Fig. 3) which indicates that one type MES-capped Au nanoclusters were synthesized independently of the reaction mixture pH.

Photoluminescent AuNCs have been reported before and several models have been proposed to explain the mechanism of PL effects. A theoretical study explains PL of nanosized noble metals by electronic transitions between the occupied d bands and states above the Fermi level [34]. Small metal nanoclusters have sizes comparable to the Fermi wavelength of electrons which result in molecular-like properties including size-dependent fluorescence [11, 35, 36]. In accordance with the free electron model a simple equation could be derived [37] for the relation between the PL emission band maxima and the quantity of gold atoms in the cluster:

$$N = \left(\frac{e\lambda_{\max} E_F}{hC} \right)^2 .$$

Here λ_{max} is the PL emission wavelength, E_F is the Fermi energy of bulk gold in eV, e is the number numerically equal to the electron charge, h is the Planck constant and c is the speed of light.

The calculation reveals that MES capped AuNCs consist of about 10 gold atoms. Theoretically it is predicted that stable nanoclusters can be formed by a specific number of gold atoms that can be characterized by a magic number [38] and the closest magic number is eight. So, we can conclude that fluorescent MES capped AuNCs could contain 8 gold atoms (Fig. 5). However, there are many possible configurations of 8 gold atom clusters [39, 40]. Matulis et al. [41] calculated possible absorption spectra of most stable Au8 isomers, using the density functional theory [44]. The three-dimensional pyramidal ($C2_v$) structure of Au8 isomer has absorption peaks at 274.3 and 418.9 nm [41] that are closest to our experimental results (275 and 420 nm, respectively (Fig. 1)). Our spectroscopic data is slightly different in comparison with the results presented by An et al. [18]. Our synthesized MES capped AuNCs have PL excitation and emission peaks at 420/480 nm, respectively (Fig. 1) and correlate with the results obtained by others: 420/485 nm [16], 420/495 nm [28], and 425/475 nm [29].

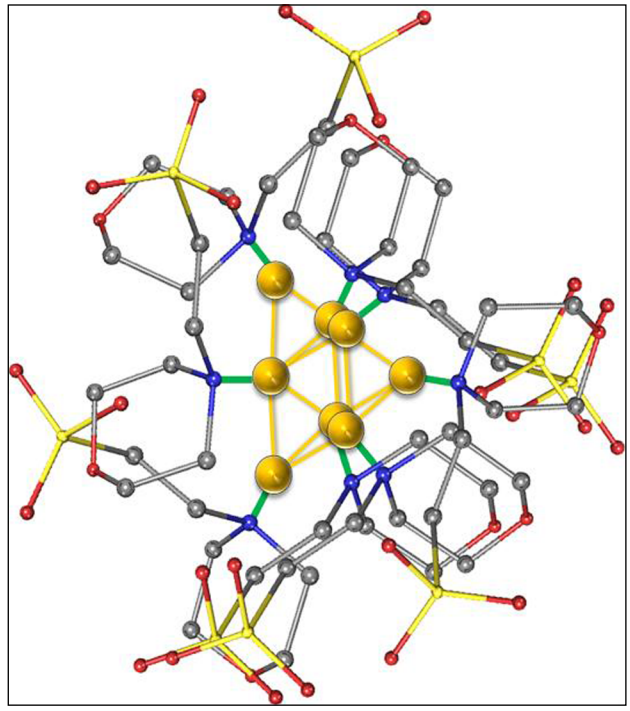

Fig. 5. Possible configuration of MES capped AuNC consisting of 8 gold atoms and 8 MES molecules (gold is dark yellow online, nitrogen is blue, oxygen is red, sulfur is light yellow, and carbon is grey)

It is possible for MES to bond with AuNCs atoms via an N atom or an O atom from the SO_3H functional group [18]. We chose to depict possible configuration of MES capped AuNC with the Au–N bond, which is more likely, because the SO_3H group ensures better solubility in water of a nanocluster (Fig. 5).

We demonstrate that absorption spectra depend on the pH value and do not coincide with the PL excitation of the solution (Figs. 4 and 1). It could be explained that in addition to the photoluminescent MES capped AuNCs containing 8 gold atoms under a chemical reaction additional non-photoluminescent nanoclusters are formed. Absorption bands at 290 and 340 nm (that were not detected in the PL excitation spectra) belong to non-photoluminescent reaction products the spectra of which strongly depend on the pH value (Fig. 4). At pH 7.5 the main absorption band peaks at 307 nm, but in an acidifying medium it shifts hypsochromically and at pH 4.9 it appears at 270 nm. A second absorption band with a peak at 340 nm can be seen in the absorption spectra together with a short wavelength absorption band shift. This peak gains the highest optical density at pH 6.1, although at both increasing and reducing pH it disappears. These changes can be explained by the size and shape variations of non-photoluminescent nanoparticles with the pH of the reaction mixture. The size of these gold particles has to be bigger than 1.5 nm (compared with the Fermi wavelength) because they do not display a PL signal while excited at both 270 and 340 nm. On the other hand, they have to be small enough, or in low concentration to not present an SPR absorption

band. According to the literature data the SPR band of gold nanoclusters appears at the size of gold nanoparticles bigger than 2 nm [43]. So, during the synthesis reaction, besides photoluminescent AuNCs, which consist of 8 atoms, another nanoparticles ranging in a size up to 2 nm are formed. These non-photoluminescent gold nanoparticles are too small to be eliminated by simple centrifugation.

In an acidic medium from pH 5.8 to 4.9, additional non-photoluminescent nanoparticles are produced that have an absorption band at 525 nm (Fig. 4). This absorption band can be attributed to the typical SPR absorption generated by large gold nanoparticles [1, 3]. These particles could be efficiently separated by centrifugation as it is seen in Fig. 4. After centrifugation, the absorption band at 525 nm disappears in the supernatant and dissolving of the pellet in the water restores it with no negative effects. Therefore, using our discussed synthesis route with an adjusted buffer pH (from pH 5 to 6), and then separating particles by centrifugation, we can produce stable MES capped plasmonic gold nanoparticles. These plasmonic nanoparticles could be used as a contrast for cell and biological imaging, as well as for photothermal therapy [44].

The size of these large gold nanoparticles could be estimated from the surface plasmon absorption band maximum position in the absorption spectra according to the Mie theory by using the Mieplot software. The theoretical calculations of the SPR absorption spectra of gold nanoparticles (Fig. 5) show that the SPR absorption band at 525 nm of MES coated gold nanoparticles synthesized at pH 5.8, 5.5, 5.2 and 4.9 could be fitted with the theoretically calculated SPR absorption band for nanoparticles with a size around 20 nm.

For pH values from pH 5.8 to 5.2 we did not register any change in the extinction peak position at 525 nm, which is as usual attributable to SPR [45, 46] (Fig. 6). It can be concluded that only one type of plasmonic nanoparticles is formed in all three cases.

The second absorption band is formed by decreasing the pH of our sample to 4.9 (Fig. 7). We have considered three possible scenarios in order to investigate the nature of this band. Firstly, it is possible that a second reaction center is activated by decreasing the pH to 4.9 and with the help of this center a second type in the size of gold nanoparticles is formed. In other words, nanoparticles of two different sizes coexist in the solution mutually. The calculated sizes of these two types of particles are 20 and 158 nm, respectively.

Another possibility is that the second band is just a quadruple mode of a single, large gold nanoparticle, which is formed after the pH is reduced. The calculated size of these particles is about 170 nm. The third possible scenario is that gold nanorods are formed after reducing the pH to 4.9. According to Link et al. [47] such nanorods should have an aspect ratio of about 2.7, and are incompatible with our modelling results. It is also known that interactions among aggregated plasmonic gold nanoparticles can produce an absorption band at around 650 nm [48], which is most likely in our case.

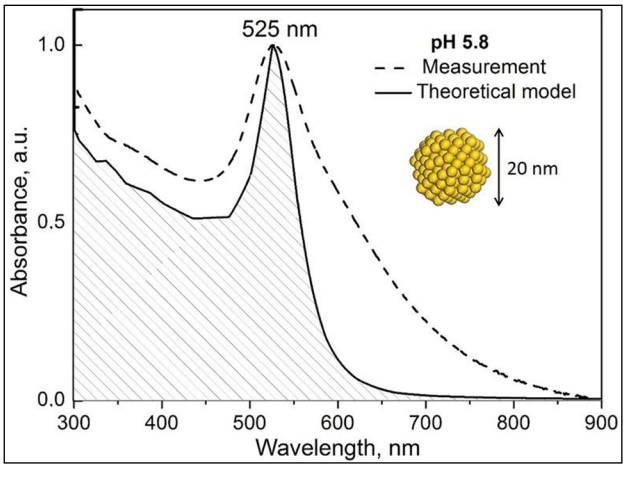

Fig. 6. Measured and theoretically calculated absorption spectra of MES capped gold nanoparticles at pH 5.8

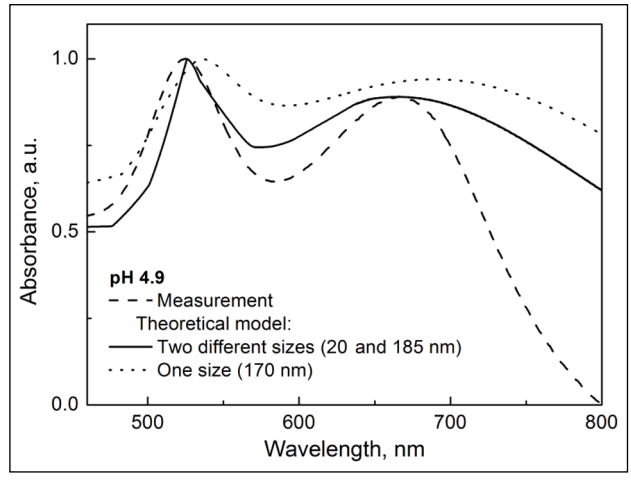

Fig. 7. Measured and theoretically calculated absorption spectra of MES coated-gold nanoparticles at pH 4.9

CONCLUSIONS

It can be concluded from our results that during the synthesis of MES capped AuNCs, three main types of particles are produced depending on the pH of the solution.

One type is photoluminescent AuNCs, the quantity of which is highest at the reaction mixture pH 6.3. On the basis of spectroscopic data, the free electron model and the density functional theory, it is calculated that the PL emitting MES capped AuNCs are formed by 8 gold atoms stacked in a three-dimensional pyramidal ($C2_V$) structure (Fig. 5). We predicted that one Au_8NC contains 8 MES molecules to bond with Au atoms via an N atom because the SO_3H group ensures better solubility in water of a nanocluster (Fig. 5).

In an acidic medium from pH 5.8 to 4.9, large gold non-photoluminescent nanoparticles are produced that have absorption bands attributed to the typical SPR absorption. These particles could be efficiently separated by centrifugation as it is seen in Fig. 4.

Absorption bands in the spectral range 250–400 nm (that were not detected in the PL excitation spectra) belong to non-photoluminescent reaction products the spectra of which strongly depend on the pH value (Fig. 4). The size of these gold particles has to be bigger than 2.0 nm (compared with the Fermi wavelength) because they do not display a PL signal while excited at 270 and 340 nm. On the other hand, they have to be small enough to not present an SPR absorption band.

ACKNOWLEDGEMENTS

This work was partly supported by the Project "Programming Cells and Management of Tumour Microenvironment for Personal Therapy in Oncology – LASTER" (VP1-3.1-ŠMM-10-V-02-027).

RK acknowledges support via a fellowship funded by the European Union Structural Funds Project "Postdoctoral Fellowship Implementation in Lithuania" within the framework of the Measure for Enhancing Mobility of Scholars and Other Researchers and the Promotion of Student Research (VP1-3.1-ŠMM-01) of the Program of Human Resources Development Action Plan.

Received 1 February 2016
Accepted 2 March 2016

References

1. K. A. Willets, R. P. Van Duyne, *Annu. Rev. Phys. Chem.*, **58**, 267 (2007).
2. A. J. Haes, C. L. Haynes, A. D. McFarland, G. C. Schatz, R. P. Duyne, S. Zou, *MRS Bull.*, **30**, 368 (2005).
3. S. Link, M. A. El-Sayed, *J. Phys. Chem. B*, **103**, 4212 (1999).
4. W. Haiss, N. T. Thanh, J. Aveyard, D. G. Fernig, *Anal. Chem.*, **79**, 4215 (2007).
5. K. H. Su, Q. H. Wei, X. Zhang, J. J. Mock, D. R. Smith, S. Schultz, *Nano Lett.*, **3**, 1087 (2003).
6. C. T. Yuan, W. C. Chou, J. Tang, et al., *Opt. Express*, **17**, 16111 (2009).
7. J. Zheng, J. T. Petty, R. M. Dickson, *J. Am. Chem. Soc.*, **125**, 7780 (2003).
8. S. W. Chen, R. S. Ingram, M. J. Hostetler, et al., *Science*, **280**, 2098 (1998).
9. S. A. Empedocles, R. Neuhauser, K. Shimizu, M. G. Bawendi, *Adv. Matter.*, **11(15)**, 1243 (1999).
10. C. L. Cheng-An, J. Lin, J. T. Hsieh, et al., *JMBE*, **29**, 276 (2009).
11. J. Zheng, C. Zhang, R. M. Dickson, *Phys. Rev. Lett.*, **93**, 077402 (2004).
12. Y. Bao, C. Zhong, D. M. Vu, J. P. Temirov, R. B. Dyer, J. S. Martinez, *J. Phys. Chem. C*, **111**, 12194 (2007).
13. H. Duan, S. Nie, *J. Am. Chem. Soc.*, **129**, 2412 (2007).
14. J. Xie, Y. Zheng, J. Y. Ying, *Am. Chem. Soc.*, **131**, 888 (2009).
15. P. Sharbari, R. J. Nikhil, *WIREs Nanomed. Nanobiotechnol.*, **6**, 102 (2014).
16. Y. Bao, H. C. Yeh, C. Zhong, et al., *J. Phys. Chem.*, **114**, 15879 (2010).
17. N. E. Good, G. D. Winget, W. Winter, T. N. Connolly, S. Izawa, R. M. M. Singh, *Biochemistry*, **5(2)**, 467 (1966).
18. W. An, L. Wintzinger, H. Turner, Y. Bao, *JOSHUA*, **7**, 24 (2010).
19. X. Xia, Y. Long, J. Wang, *Anal. Chim. Acta*, **772**, 81 (2013).
20. N. K. Pal, C. Kryschi, *Phys. Chem. Chem. Phys.*, **17**, 21423 (2015).
21. M. Rarrag, M. Tschurl, U. Heiz, *Chem. Mater.*, **25**, 862 (2013).
22. X. Mu, L. Qi, P. Dong, J. Qiao, J. Hou, Z. Nie, H. Ma, *Biosens. Bioelectron.*, **49**, 249 (2013).
23. K. G. Stamplecoskie, P. V. Kamat, *JACS*, **136**, 11093 (2014).
24. H. Wei, Z. Wang, L. Yang, S. Tian, C. Hou, Y. Lu, *Analyst*, **135**, 1406 (2010).
25. L. Chen, C. Wang, Z. Yuan, H. Chang, *Anal. Chem.*, **87**, 216 (2015).
26. H. H. Wang, C. A. Lin, C. H. Lee, et al., *ACS Nano*, **5**, 4337 (2011).
27. L. Shang, R. M. Dorlich, S. Brandholt, et al., *Nanoscale*, **3**, 2009 (2011).
28. Y. Bao, L. Wintzinger, C. H. Turner, W. A. An, *Nano LIFE*, **1**, 133 (2010).
29. H. C. Yeh, S. K. Jaswinder, J. S. Martinez, J. H. Werner, H. Yoo, *Proceedings of SPIE Photonics West*, San Francisco (2010).
30. R. Kubiliute, A. Slektaite, M. Burkanas, R. Grigiene, R. Rotomskis, *Proceedings of 9th International Conference on Medical Physics in the Baltic States*, Kaunas (2011).
31. M. Matulionyte, R. Marcinonyte, R. Rotomskis, *J. Biomed. Opt.*, **20(5)**, 051018 (2015).
32. R. Rotomskis, *Tumori*, **94**, 200 (2008).
33. P. Chylek, C. F. Bohren, R. Huffman, *Appl. Opt.*, **25**, 3166 (1986).
34. P. Appel, R. Monreal, S. Lundqvist, *Phys. Scripta*, **38(2)**, 174 (1988).
35. C. Huang, Z. Yang, K. Lee, H. Chang, *Angew. Chem.*, **119**, 6948 (2007).
36. N. Schaeffer, B. Tan, C. Dickinson, et al., *Chem. Commun.*, **34**, 3986 (2008).
37. J. Zheng, P. R. Nicovich, R. M. Dickson, *Rev. Phys. Chem.*, **58**, 409 (2007).
38. M. K. Harbola, *Proc. Natl. Acad. Sci. USA*, **89**, 1036 (1992).
39. M. Diefenbach, K. S. Kim, *J. Phys. Chem. B*, **110**, 21639 (2006).
40. R. M. Olson, M. S. Gordon, *J. Phys. Chem.*, **126(21)**, 214310 (2007).
41. V. E. Matulis, D. M. Palagin, O. A. Ivashkevich, *Russ. J. Gen. Chem.*, **80(6)**, 1078 (2010).
42. E. R. Stratmann, G. E. Scuseria, M. J. Frisch, *J. Phys. Chem.*, **109(19)**, 8217 (1998).
43. C. J. Lin, T. Yang, C. Lee, et al., *ACS NANO*, **3(2)**, 395 (2009).
44. X. Huang, M. A. El-Sayed, *AJM*, **47(1)**, 1 (2011).

45. M. Hu, J. Chen, Z. Y. Li, et al., *Chem. Soc. Rev*., **35**, 1084 (2006).
46. S. Eustis, M. A. el-Sayed, *Chem. Soc. Rev*., **35**, 209 (2006).
47. S. Link, M. B. Mohamed, M. A. El-Sayed, *J. Phys. Chem. B*, **103**, 3073 (1999).
48. H. Ahsan, T. Masaaki, W. Yingguang, *Chem. Soc. Jpn*., **78**, 262 (2005).

Akvilė Šlėktaitė, Reda Kubiliūtė, Deividas Sabonis, Ričardas Rotomskis

AUKSO NANOKLASTERIŲ, MODIFIKUOTŲ MORFOLINO LIGANDU, SPEKTRINIŲ IR ERDVINIŲ SAVYBIŲ SĄRYŠIAI

S a n t r a u k a

Pastaraisiais metais aukso nanodalelės daugiausiai dėmesio sulaukė dėl jų paviršiuje susidarančio ir nuo dalelių dydžio priklausančio plazmonų rezonanso efekto. Nanodalelėms sumažėjus iki 2 nm šis reiškinys išnyksta, o dalelės įgauna naujų savybių. Tokios aukso nanodalelės vadinamos aukso nanoklasteriais ir elgiasi panašiai kaip molekulės su diskrečiais elektroniniais lygmenimis bei nuo dydžio priklausoma fotoluminescencija. Tai suteikia galimybę nanoklasterius pritaikyti fluorescenciniame vaizdinime bei kuriant biologinius ir biocheminius jutiklius.

Darbe pristatome aukso nanoklasterių, susintetintų naudojant 2-(N-morfolino)etanesulfoninę rūgštį kaip stabilizuojantį agentą, spektrines savybes ir jų sąryšius su dalelių erdvinėmis charakteristikomis. Mes tyrėme spektrinius pokyčius, atsirandančius keičiant sintezės Ph bei naudojant skirtingus bandinių paruošimo metodus, ir pastebėjome, kad esant pH 6,3 gaunamas didžiausias fotoluminescencijos intensyvumas. Atsižvelgdami į teorinius modeliavimus nustatėme, kad šios dalelės yra sudarytos iš 8 atomų, susijungusių į trijų dimensijų piramidinę struktūrą ($C2_V$). Itin rūgštinėje terpėje (pH 4,9–5,8) susidarė papildomos plazmoninėmis savybėmis pasižyminčios dalelės, kurių apskaičiuotas dydis buvo apie 20 nm.